

## Article

# Carbon-Silica Composite as Adsorbent for Removal of Hazardous C.I. Basic Yellow 2 and C.I. Basic Blue 3 Dyes

Małgorzata Wiśniewska <sup>1,\*</sup>, Monika Wawrzekiewicz <sup>2</sup>, Magda Onyszko <sup>2</sup>, Magdalena Medykowska <sup>1</sup>, Agnieszka Nosal-Wiercińska <sup>3</sup> and Viktor Bogatyrov <sup>4</sup>

<sup>1</sup> Department of Radiochemistry and Environmental Chemistry, Faculty of Chemistry, Institute of Chemical Sciences, Maria Curie-Skłodowska University in Lublin, M. Curie-Skłodowska Sq. 3, 20-031 Lublin, Poland; m.medykowska@poczta.umcs.lublin.pl

<sup>2</sup> Department of Inorganic Chemistry, Faculty of Chemistry, Institute of Chemical Sciences, Maria Curie-Skłodowska University in Lublin, M. Curie-Skłodowska Sq. 2, 20-031 Lublin, Poland; m.wawrzekiewicz@poczta.umcs.lublin.pl (M.W.); m.tarczyluk97@gmail.com (M.O.)

<sup>3</sup> Department of Analytical Chemistry, Faculty of Chemistry, Institute of Chemical Sciences, Maria Curie-Skłodowska University in Lublin, M. Curie-Skłodowska Sq. 3, 20-031 Lublin, Poland; anosal@poczta.umcs.lublin.pl

<sup>4</sup> Chuiko Institute of Surface Chemistry, National Academy of Sciences of Ukraine, General Naumov Street 17, 03164 Kyiv, Ukraine; vbogat@ukr.net

\* Correspondence: wisniewska@hektor.umcs.lublin.pl



**Citation:** Wiśniewska, M.; Wawrzekiewicz, M.; Onyszko, M.; Medykowska, M.; Nosal-Wiercińska, A.; Bogatyrov, V. Carbon-Silica Composite as Adsorbent for Removal of Hazardous C.I. Basic Yellow 2 and C.I. Basic Blue 3 Dyes. *Materials* **2021**, *14*, 3245. <https://doi.org/10.3390/ma14123245>

Academic Editors: Alain Celzard and Dusan Losic

Received: 24 April 2021

Accepted: 9 June 2021

Published: 11 June 2021

**Publisher's Note:** MDPI stays neutral with regard to jurisdictional claims in published maps and institutional affiliations.



**Copyright:** © 2021 by the authors. Licensee MDPI, Basel, Switzerland. This article is an open access article distributed under the terms and conditions of the Creative Commons Attribution (CC BY) license (<https://creativecommons.org/licenses/by/4.0/>).

**Abstract:** Treatment of wastewaters containing hazardous substances such as dyes from the textile, paper, plastic and food industries is of great importance. Efficient technique for the removal of highly toxic organic dyes is adsorption. In this paper, adsorptive properties of the carbon-silica composite (C/SiO<sub>2</sub>) were evaluated for the cationic dyes C.I. Basic Blue 3 (BB3) and C.I. Basic Yellow 2 (BY2). The sorption capacities were determined as a function of temperature (924.6–1295.9 mg/g for BB3 and 716.3–733.2 mg/g for BY2 at 20–60 °C) using the batch method, and the Langmuir, Freundlich and Temkin isotherm models were applied for the equilibrium data evaluation using linear and non-linear regression. The rate of dye adsorption from the 100 mg/L solution was very fast, after 5 min. of phase contact time 98% of BB3 and 86% of BY2 was removed by C/SiO<sub>2</sub>. Presence of the anionic (SDS), cationic (CTAB) and non-ionic (Triton X-100) surfactants in the amount of 0.25 g/L caused decrease in BB3 and BY2 uptake. The electrokinetic studies, including determination of the solid surface charge density and zeta potential of the composite suspensions in single and mixed adsorbate systems, were also performed. It was shown that presence of adsorption layers changes the structure of the electrical double layer formed on the solid surface, based on the evidence of changes in ionic composition of both surface layer and the slipping plane area. The greatest differences between suspension with and without adsorbates was obtained in the mixed dye + SDS systems; the main reason for this is the formation of dye-surfactant complexes in the solution and their adsorption at the interface.

**Keywords:** dyes removal; basic blue 3; basic yellow 2; adsorption; composite; wastewater treatment

## 1. Introduction

Industrial wastewater is one of the most dangerous sources of environmental pollution. The rapid expansion of industrial production, which uses large amounts of water, has contributed significantly to pollution and, in many cases, contamination of surface waters [1]. The group of industrial wastewaters that poses serious problems in its disposal includes wastewater-containing dyes, which are difficult to decompose and poorly biodegradable. In addition, their presence significantly deteriorates the color of the wastewater, and even small concentrations in the environment cause change in the color of water reservoirs. Strong coloration of water significantly reduces light transmission, and thus the process of the photosynthesis of aquatic plants, and limits self-purification of water. Moreover,

most dyes have a negative effect on aquatic animals, mainly fish and plankton. Indirect impact is related to the deterioration of living conditions by changing the light exposure and water composition. The direct effect, on the other hand, is based on the poisonous properties of some dyes [2]. Difficulties in developing an economical, effective and simple method of dye removal are caused by rapid changes in the production technology and the use of various dyes in the technological process. The main sources of dyes in industrial wastewater are the following plants: organic dyes production, textile, leather and paper industries, plastics, food, petroleum, printing and cosmetics industries.

One of the available methods of water purification from heavy metal ions is adsorption [3]. Due to the highly developed surface area (even a few thousands of  $\text{m}^2/\text{g}$ ) and porous structure, as well as favorable surface properties, carbon materials (carbon nanotubes, graphene oxide and activated carbon) are perfectly suited as effective and selective adsorbents. Their adsorptive properties can be additionally modified by formation of composites with other compounds. These combined materials composed of two or more constituents have specific characteristics and better properties than individual components.

Adsorbents containing carbon such as carbon nanotubes, activated carbon, biochar, graphene, carbon nanofibers and its derivatives are widely used in the process of removal of undesirable, toxic and hazardous substances (such as heavy metal ions, dyes, pesticides, drugs, polymers, surfactants) from aqueous solutions [4–11]. The kind of adsorption depends on the type of surface functional groups on the carbon materials and their interactions with adsorbate molecules. The main mechanisms include: ion exchange, chemical bonding, electrostatic interaction, surface complexation, surface precipitation and physical adsorption [12].

The interesting type of adsorbents are the composites of carbon with inorganic oxides (such as  $\text{SiO}_2$ ,  $\text{Al}_2\text{O}_3$  and  $\text{TiO}_2$ ) or metallic elements (such as Si/C/Mn/Fe and Si/C/Mn). Previously performed studies confirmed the usefulness of the hybrid carbon-mineral nanocomposites with metallic elements (especially Si/C/Mn) for the adsorption removal of Cu(II) ions from aqueous solution in poly(acrylic acid) presence [13]. In turn, the carbon-silica composite showed high efficiency of Cu(II) adsorption from the solution containing proteins with different internal stability (ovalbumin and lysozyme) [14], as well as ionic polyacrylamides [15].

In the present study, the sorption properties of carbon-silica composite for the cationic dyes, i.e., C.I. Basic Yellow 2 and C.I. Basic Blue 3 from liquid phase, were examined. The dyes are used mainly in the textile industry, so large amounts are present in textile effluents. C.I. Basic Yellow 2 is used for silk, acrylic, tannin mordant dyeing, and also can be used for leather, paper, hemp and glue coloring. It can also be found in oil and fat, paint color, and ink. C.I. Basic Blue 3 is applied for wool/nitriles and stick/acrylic blended fabric dyeing, as well as for direct printing of acrylic carpets. That is why their effective removal is highly necessary due to the intense color of these substances and effluents. Basic dyes show significant toxicity to living organisms, especially mutagenic and carcinogenic effects [16,17]. The mechanisms of these dyes removal were characterized based on analysis of the sorption capacities, solid surface charge density and zeta potential in the presence of surfactant with different ionic character (cationic CTAB, anionic SDS and nonionic Triton X-100). The conducted research undoubtedly enriched the knowledge about the possibility of using an innovative carbon-silica composite for dye removal. So far, its suitability for separation of heavy metal ions and polymers (both natural and synthetic) has been examined [14,15]. This paper describes for the first time the use of C/SiO<sub>2</sub> composite for adsorptive removal of basic dyes.

## 2. Materials and Methods

### 2.1. Composite and Dyes

Pyrogenic silica A-300 (Pilot plant of Institute of Surface Chemistry NAN of Ukraine, Kalush) and phenol-formaldehyde resin of novolac type (JSC 'Ukrainian resins') were used for composite synthesis. Both components were mixed in a weight ratio of 1:1 and

ground by a porcelain ball mill for 2 h. Next these reagents were subjected to pyrolysis in argon flow at 800 °C for 2 h. The detailed textural and surface characteristics of obtained C/SiO<sub>2</sub> composite was presented in previous paper [14]. The obtained product contains 31.5% (by weight) of carbon, has a specific surface area ( $S_{BET}$ ) equal to 297 m<sup>2</sup>/g and mean pore diameter—6.1 nm. The particle size distribution of C/SiO<sub>2</sub> composite was measured using Zetameter Nano ZS apparatus (Malvern Instruments, Malvern, UK) and is presented in Figure 1. The mean diameter of solid aggregates in 0.001 mol/L NaCl supporting electrolyte solution was about 790 nm.

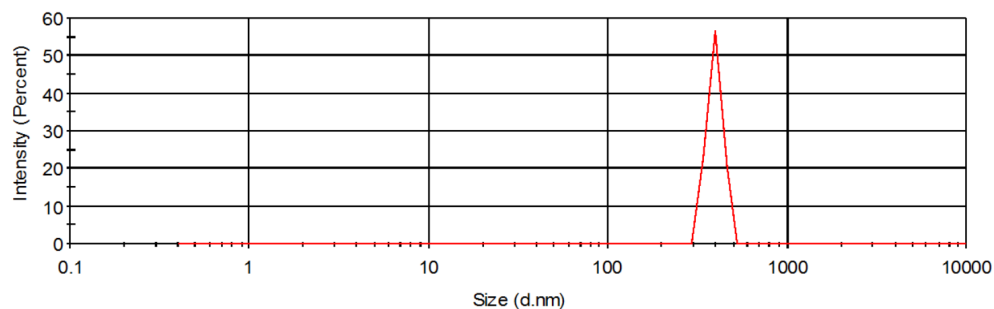


**Figure 1.** Particle size distribution of C/SiO<sub>2</sub> composite.

The morphology of the C/SiO<sub>2</sub> composite surface was observed using electron microscopes: scanning electron microscope (SEM) Quanta<sup>TM</sup> 3D FEG (FEI Company, Hillsboro, OR, USA) and transmission electron microscope (TEM) Tecnai<sup>TM</sup> G2 20 (FEI Company, Hillsboro, OR, USA). The appropriate detectors (EDS, EDX) cooperating with the microscopes enables the determination of element composition in the adsorbent phase. The images of C/SiO<sub>2</sub> composite surface are presented in Figure 2. Analysis of the microscopic images reveals that the composite has a disordered structure in which the individual components are randomly distributed.

C.I. Basic Yellow 2 and C.I. Basic Blue 3 properties are presented in Figure 3. The dyes were purchased from Classic Dyestuff Inc. (High Point, NC, USA). The stock solutions of BY2 and BB3 of the initial concentration  $C_0 = 1000$  mg/L were prepared. The working solutions were prepared by diluting the stock solution in the presence of 0.001 mol/L NaCl as supporting electrolyte.

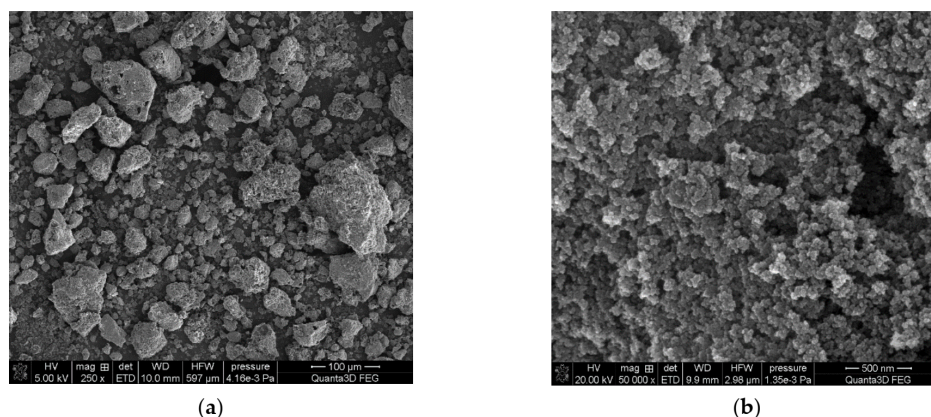


**Figure 2.** Cont.

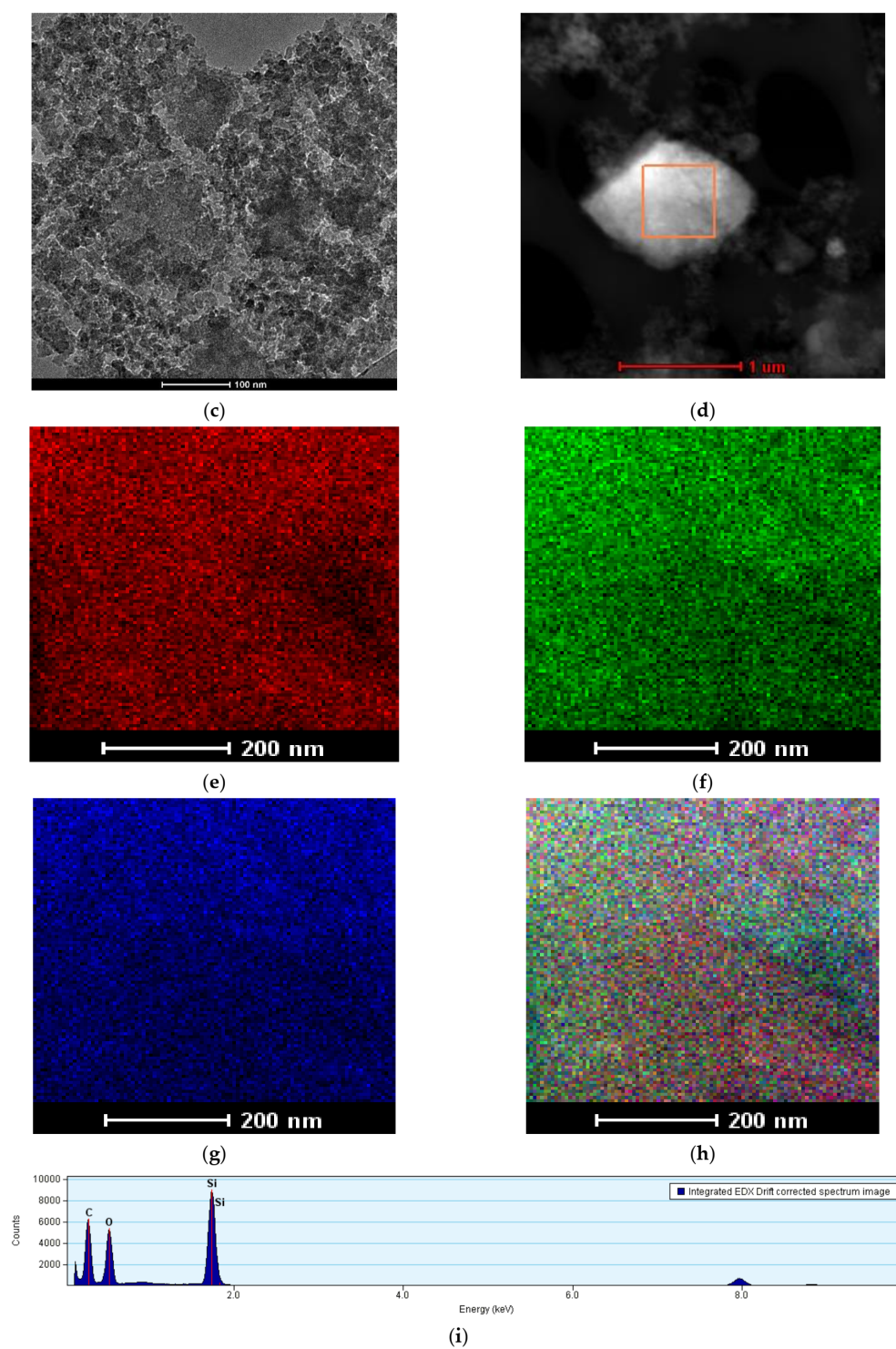


**Figure 2.** (a–b) SEM and (c–d) TEM images of C/SiO<sub>2</sub> composite as well as TEM maps of (e) carbon, (f) silicon, (g) oxygen, (h) composite and (i) integrated EDX drift corrected spectrum.

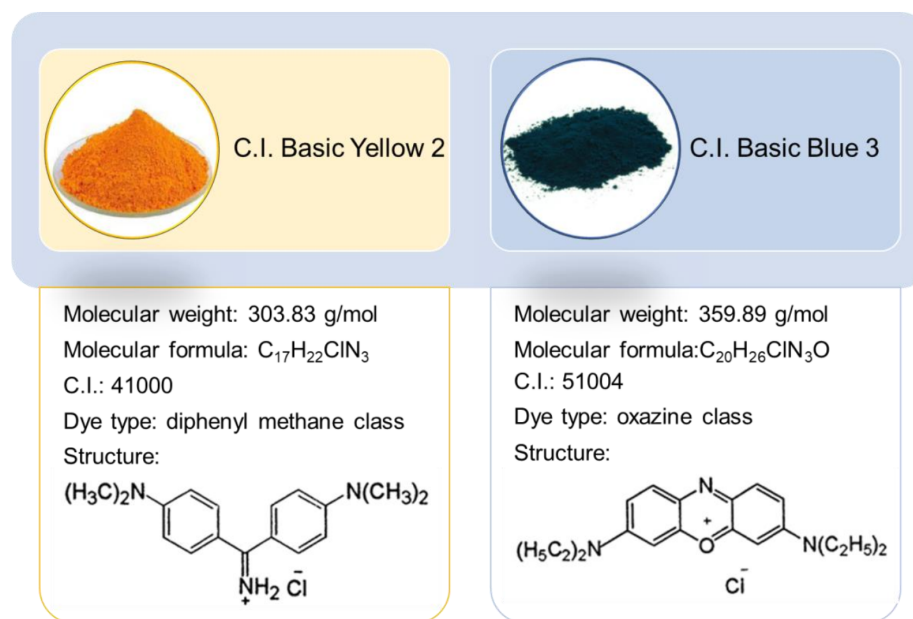


Figure 3. Dyes characteristics.

Surface active agents such as anionic sodium dodecyl sulphate (SDS), non-ionic 2-[4-(2,4,4-trimethylpentan-2-yl)phenoxy]ethanol (Triton X-100) and cationic hexadecyltrimethylammonium bromide (CTAB) of laboratory grade were purchased from Sigma-Aldrich (Darmstadt, Germany). Sodium chloride and hydroxide were obtained from Avantor Performance Materials Poland S.A. (Gliwice, Poland).

## 2.2. Adsorption Studies

In the batch adsorption experiment, 0.02 g of C/SiO<sub>2</sub> was added to 20 mL of an aqueous dye solution and shaken using an Elpin 358+ (Elpin, Lubawa, Poland) laboratory shaker at 180 cycle/min. for 24 h (equilibrium experiment) at 20, 40 and 60 °C or from 1 to 240 min. (kinetic experiment) at 20 °C. The initial BY2 or BB3 concentrations used to collect isotherm data were ranged from 100 to 1000 mg/L. In order to calculate kinetic parameters in C/SiO<sub>2</sub>-BY2 and C/SiO<sub>2</sub>-BB3 systems, a dye solution with an initial concentration equal to 100 mg/L was prepared. Impact of surfactants such as SDS, CTAB and TX100 on the dye's uptake by C/SiO<sub>2</sub> after sorption time  $t = 60$  min was investigated in the systems containing 100 mg/L of the dye and 0.25 g/L of SDS, TX100 or CTAB. The amounts of BY2 or BB3 adsorbed by C/SiO<sub>2</sub> at equilibrium ( $q_e$ ) and at time  $t$  ( $q_t$ ) were calculated from the following formulas:

$$q_e = \frac{(C_0 - C_e)}{m} \times V \quad (1)$$

$$q_t = \frac{(C_0 - C_t)}{m} \times V \quad (2)$$

where:  $C_0$ ,  $C_e$  and  $C_t$  (mg/L)—dyes concentrations in the solution before adsorption, at equilibrium and after sorption time  $t$ , respectively,  $V$  (L)—volume of the solution, and  $m$  (g)—mass of C/SiO<sub>2</sub>.

Dye solutions were filtered after sorption experiments and dyes concentrations were measured using the UV-Vis spectrophotometry Cary 60 (Agilent, Santa Clara, CA, USA) at the maximum wavelengths 430 nm and 645 nm for BY2 and BB3, respectively. All adsorption experiments were performed in triplicate, and the mean values have been used for data evaluation. The standard deviation did not exceed 3%.

### 2.2.1. Isotherm Studies

The equilibrium adsorption data of BY2 and BB3 on C/SiO<sub>2</sub> composite were analyzed by calculation of isotherm parameters. The Langmuir, Freundlich and Temkin isotherm equations were taken into account using their linear and non-linear forms which are presented in Table 1 [18–20]. The Langmuir isotherm model suggests that adsorbate uptake occurs on a homogeneous surface of adsorbent, forming a monolayer without interaction between adsorbed molecules. The Freundlich and Temkin isotherm models consider surface heterogeneity and the interactions between adsorbents and adsorbates. One of the assumptions of Temkin's model is that the heat of adsorption of all molecules in the layer decreases linearly.

**Table 1.** Isotherm models used for description of BY2–C/SiO<sub>2</sub> and BB3–C/SiO<sub>2</sub> systems.

Isotherm	Equation No.	Non-Linear Forms	Linear Forms
Langmuir	(3)–(4)	$q_e = \frac{k_L Q_0 C_e}{1 + C_e k_L}$	$\frac{C_e}{q_e} = \frac{1}{Q_0 k_L} + \frac{C_e}{Q_0}$
Freundlich	(5)–(6)	$q_e = k_F C_e^{1/n}$	$\log q_e = \log k_F + \frac{1}{n} \log C_e$
Temkin	(7)–(8)	$q_e = \frac{RT}{b_T} \ln A C_e$	$q_e = \left(\frac{RT}{b_T}\right) \ln A + \left(\frac{RT}{b_T}\right) \ln C_e$

where:  $q_e$ —the amount of basic dye adsorbed per unit mass of C/SiO<sub>2</sub> at equilibrium (mg/g),  $C_e$ —the equilibrium concentration of solution (mg/L),  $Q_0$ —the monolayer adsorption capacity (mg/g),  $k_L$ —the Langmuir constant (related to the free energy of adsorption) (L/mg),  $k_F$  (mg<sup>1–1/n</sup> L<sup>1/n</sup>/g) and  $1/n$ —the Freundlich constants connected with adsorption capacity of adsorbent and the surface heterogeneity, respectively,  $R$ —the gas constant (8.314 J/mol K),  $T$ —the temperature (K),  $A$  (L/g) and  $b_T$  (J/mol)—the Temkin constants.

Applying linear regression, the isotherm parameters were calculated from the slopes and intercepts of the  $C_e/q_e$  vs.  $C_e$ ,  $\log q_e$  vs.  $\log C_e$  and  $q_e$  vs.  $\ln C_e$  plots ( $Q_0 = 1/\text{slope}$ ,  $b = \text{slope}/\text{intercept}$ ,  $1/n = \text{slope}$ ,  $k_F = 10^{\text{intercept}}$ ,  $b_T = RT/\text{slope}$ ,  $A = \exp(\text{intercept}/\text{slope})$ ). Microsoft Excel 2013 with the Solver add-in was used for calculation of the above mentioned parameters by non-linear regression. Calculation of the values of determination coefficients ( $R^2$ ), adjusted R-squared ( $\text{adj-}R^2$ ) and Marquardt's percent standard deviation (MPSD) enable an assessment of the best fit of the experimental data.  $\text{adj-}R^2$  is usually used to compare model of different sizes; in contrast to  $R^2$ , it can go up or down when a variable is taken out of the model. These parameters were calculated from the following Equations (9)–(11) [19,20]:

$$R^2 = 1 - \frac{\sum (q_{e \text{ exp}} - q_{e \text{ cal}})^2}{\sum (q_{e \text{ exp}} - q_{e \text{ mean}})^2} \quad (9)$$

$$R^2_{\text{adj}} = 1 - \left[ \frac{(1 - R^2)(n - 1)}{n - k - 1} \right] \quad (10)$$

$$\text{MPSD} = \sum_{i=1}^n \left( \frac{q_{e \text{ exp}} - q_{e \text{ cal}}}{q_{e \text{ exp}}} \right)^2 \quad (11)$$

where:  $q_{e \text{ exp}}$  (mg/g)—amount of acid dyes sorbed at equilibrium,  $q_{e \text{ cal}}$  (mg/g)—amount of acid dyes sorbed calculated from the non-linear models,  $q_{e \text{ mean}}$  (mg/g)—measured by the mean of  $q_{e \text{ exp}}$  values,  $n$ —number of points in data sample,  $k$ —number of independent regressors.

### 2.2.2. Thermodynamic Studies

The thermodynamic parameters of BB3 and BY2 adsorption on C/SiO<sub>2</sub> were calculated at three different temperatures using the Equations:

$$\Delta G^0 = -RT \ln K_c c^0 \quad (12)$$

$$K_c = \frac{q_e}{C_e} \quad (13)$$

$$\ln K_c c^0 = \frac{\Delta S^0}{R} - \frac{\Delta H^0}{RT} \quad (14)$$

where  $\Delta G^0$ —change of free energy of the system (kJ/mol),  $\Delta H^0$ —change of free enthalpy of the system (kJ/mol),  $\Delta S^0$ —change of free entropy of the system (kJ/mol K),  $R$ —gaseous constant (8.314 J/mol K),  $T$ —temperature (K),  $K_c$ —distribution constant at equilibrium (L/g),  $c^0 \equiv 1000$  g/L [21],  $q_e$ —the amount of basic dye adsorbed per unit mass of C/SiO<sub>2</sub> at equilibrium (mg/g),  $C_e$ —the equilibrium concentration of solution (mg/L).

### 2.3. Electrokinetic Studies

The electrokinetic measurements included determination of the solid surface charge density ( $\sigma_0$ ) and zeta potential ( $\zeta$ ) of the systems without and containing dyes or dye + surfactant mixture in the supporting electrolyte solution (0.001 mol/L NaCl). The following suspensions were examined: C/SiO<sub>2</sub> + NaCl, C/SiO<sub>2</sub> + NaCl + D, C/SiO<sub>2</sub> + NaCl + D + CTAB, C/SiO<sub>2</sub> + NaCl + D + SDS and C/SiO<sub>2</sub> + NaCl + D + TX-100 (where D: BY2 or BB3). The concentration of the dyes were 100 mg/L, whereas that of the surfactants were 0.25 g/L.

A potentiometric titration method was applied to the determination of surface charge density of the examined systems and their points of zero charge (pzc). The pzc is at such pH value at which the concentration of positively and negatively charged surface groups is the same and thus  $\sigma_0 = 0$ . Dependencies of  $\sigma_0$  as a function of solution pH (changing in the range 3–11) were calculated by the special software “titr\_v3” [22]. The examined solution (of volume 50 mL) was introduced to the Teflon vessel thermostated (20 °C) using thermostat RE 204 (Lauda, Germany). The glass and calomel electrodes (Beckman Instruments) as well as pH-meter PHM 240 (Radiometer, Sweden) were used to continuous control of system’s pH during titration, which was performed by the use of automatic microburette Dosimat 765 (Metrohm, Switzerland) and computer. The examined systems were titrated with NaOH solution of concentration 0.1 mol/L and the applied solid mass was 0.1 g.

Electrophoretic mobility ( $u_e$ ) measurements allowed the determination of zeta potential ( $\zeta$ ) of carbon-based silica particles (Zetameter Nano ZS, Malvern Instruments, Malvern, UK) based on the Henry’s equation [23]. Moreover, the determination of isoelectric points (iep) of the solid is possible. It is at a pH value at which the concentration of positively and negatively charged groups/ions in the slipping plane area is the same and thus  $\zeta = 0$ . The suspensions were prepared by addition of 0.02 g of the C/SiO<sub>2</sub> composite to 200 mL of the supporting electrolyte solution without or containing one or mixed adsorbates. This prepared system was sonicated for 3 min and divided into several parts, differing in the pH value (changing in the range 2–10). Next the electrophoretic mobility of each sample was measured using dip cell in the cycles of five repetitions. Electrokinetic measurements were performed in fivefold and the mean values have been used for data estimation. The standard deviation did not exceed 3%.

## 3. Results

### 3.1. Isotherm Studies

The equilibrium adsorption data describing BY2 and BB3 adsorption on C/SiO<sub>2</sub> presented in Figure 4 were analyzed by using the linear and non-linear forms of three popular isotherm models. The isotherm parameters were calculated and are listed in Tables 2 and 3.

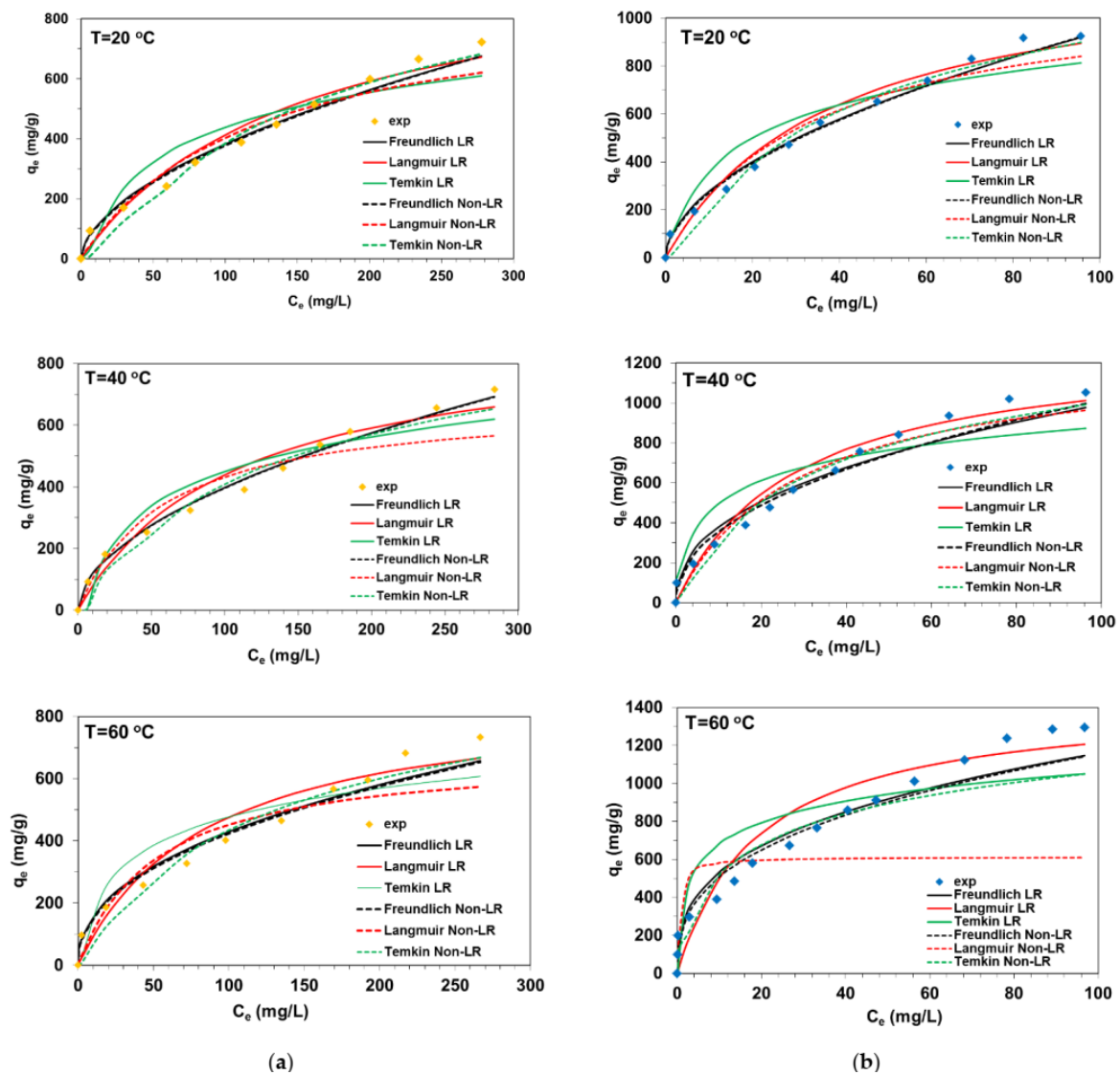


**Figure 4.** Equilibrium adsorption data in (a) BY2-C/SiO<sub>2</sub> and (b) BB3-C/SiO<sub>2</sub> systems at different temperatures (where: LR—linear regression, Non-LR—non-linear regression).

**Table 2.** Parameters of the Freundlich, Langmuir, and Temkin isotherm models calculated for the adsorption systems at 20–60 °C using linear regression.

Model	Parameters	BY2			BB3		
		Temperature (°C)					
		20	40	60	20	40	60
Langmuir	$Q_0$ (mg/g)	1038.8	905.7	878.5	1252.3	1308.9	1443.2
	$k_L$ (L/mg)	0.007	0.010	0.012	0.026	0.035	0.053
	$R^2$	0.836	0.904	0.876	0.904	0.901	0.914
Freundlich	$k_F$ (mg <sup>1-1/n</sup> L <sup>1/n</sup> /g)	29.32	34.50	58.11	81.56	144.25	243.99
	$1/n$	0.558	0.531	0.434	0.531	0.419	0.338
	$R^2$	0.977	0.991	0.970	0.984	0.948	0.946
Temkin	$b_T$ (J g/mol mg)	14.77	15.23	18.64	12.38	14.86	15.22
	$A$ (L/mg)	0.137	0.160	0.362	0.608	1.952	6.565
	$R^2$	0.838	0.894	0.812	0.847	0.760	0.773



**Table 3.** Parameters of the Freundlich, Langmuir, and Temkin isotherm models calculated for the adsorption systems at 20–60 °C using non-linear regression.

Model	Parameters	BY2			BB3		
		Temperature (°C)					
		20	40	60	20	40	60
Langmuir	$Q_0$ (mg/g)	891.8	680.8	686.3	1134.1	1251.7	613.5
	$k_L$ (L/mg)	0.008	0.017	0.019	0.030	0.035	1.75
	MPSD	0.405	0.255	0.699	0.504	0.949	2.350
	$R^2$	0.946	0.897	0.874	0.964	0.962	0.471
	$R^2_{adj}$	0.930	0.867	0.838	0.956	0.954	0.383
Freundlich	$k_F$ (mg <sup>1-1/n</sup> L <sup>1/n</sup> /g)	27.37	34.09	55.41	77.70	124.55	223.25
	1/n	0.570	0.533	0.442	0.543	0.456	0.357
	MPSD	0.0879	0.032	0.109	0.083	0.287	0.365
	$R^2$	0.991	0.993	0.978	0.994	0.983	0.970
	$R^2_{adj}$	0.988	0.991	0.971	0.992	0.979	0.965
Temkin	$b_T$ (J g/mol mg)	8.51	10.59	10.42	7.57	7.95	10.52
	$A$ (L/mg)	0.038	0.058	0.062	0.163	0.249	0.891
	MPSD	0.936	0.988	1.004	0.999	1.059	1.352
	$R^2$	0.977	0.961	0.958	0.982	0.970	0.915
	$R^2_{adj}$	0.971	0.950	0.946	0.977	0.964	0.901

Analyzing equilibrium data presented in Figure 2, the preferential adsorption of BB3 by C/SiO<sub>2</sub> can be seen. The sorption capacities of C/SiO<sub>2</sub> determined experimentally ( $q_{e\text{ exp}}$ ) for BB3 were found to be 924.6 mg/g, 1052.1 mg/g and 1295.9 mg/g at 20, 40 and 60 °C, respectively. Insignificant impact of temperature on the BY2 uptake was observed, the values of  $q_{e\text{ exp}}$  were ranged from 716.3 mg/g to 733.2 mg/g at 20–60 °C. The sorption capacities of the composite for BB3 and BY2 were compared with data available in the literature [17,24–31] and are presented in Table 4. In addition, many valuable reports can be found in the literature on the adsorptive removal of dyes of different types using composites [32–36]. It is worth mentioning here that attempts to remove BB2 and BB3 from model solutions and wastewater were made using the following methods: electrocoagulation [37], electrolysis [38], photocatalysis [39], oxidation [40], or sonification [41].

**Table 4.** Comparison of adsorption capacity of different adsorbents towards BB3 and BY2.

Kind of Adsorbent	$q_e$ (mg/g)		Ref.
	BB3		
Durian peel	49.5		[24]
Chitosan-based adsorbent	166.5		[25]
Sulfuric acid-activated montmorillonite	277		[26]
Fe <sub>3</sub> O <sub>4</sub>	7.474		-
PANI (polyaniline)	47.977		[17]
PANI/Fe <sub>3</sub> O <sub>4</sub> composite	78.13		-
C/SiO <sub>2</sub> composite	925–1296		This study
BY2			
Natural untreated clay (Pasinler clay, originating from the eastern of Turkey)	833.3		[27]
Manure ash	1428.6		[28]
Granular activated carbon	598.8		[29]
Bagasse fly ash	31.17		[30]
Mesoporous carbon oxidized at 30–60 °C	172–355.2		[31]
C/SiO <sub>2</sub> composite	716–733		This study

Comparing the Freundlich isotherm parameter  $k_F$  determined in BB3-C/SiO<sub>2</sub> and BY2-C/SiO<sub>2</sub> systems with the linear (29.32–243.99 mg<sup>1-1/n</sup> L<sup>1/n</sup>/g) and non-linear

( $27.37\text{--}223.25 \text{ mg}^{1-1/n} \text{ L}^{1/n}/\text{g}$ ) regression, it was found that these values are close to each other. Tables 2 and 3 show that  $1/n$  heterogeneity factors are below 1 which means a favorable adsorption of a physical nature during the basic dye adsorption on the composite (e.g., hydrogen bonds between N atoms of the dyes and  $-\text{OH}$  or  $-\text{OH}_2^+$  groups present on composite surface) [42,43]. The Marquardt's percent standard deviation values varied from 0.032 to 0.365 and were the smallest precisely for the Freundlich model. Even though the Freundlich model gives better comparative numerical results (in terms of deviations), visual analysis of the data reveals that it is still only an approximation of the actual process characteristics. The values of the Langmuir isotherm parameters corresponding to the monolayer coverage of adsorbate on the adsorbent surface ( $Q_0$ ) and free energy of adsorption ( $k_L$ ) determined by the linear and non-linear method were significantly different from each other. Based on the comparison of the  $R^2$ , adj- $R^2$  and MPSD values, it can be stated that the Langmuir model does not adequately describe the adsorption systems under discussion. The Temkin model also cannot be used to describe the adsorption systems. The non-linear regression is more appropriate for the evaluation of isotherm parameters than the linear regression in the BB3-C/SiO<sub>2</sub> and BY2-C/SiO<sub>2</sub> systems.

### 3.2. Thermodynamic Parameters

To study the feasibility of BB3 and BY2 adsorption on the composite, the thermodynamic parameters such as free energy, enthalpy and entropy changes were calculated from Equations (12) and (13). The entropy and enthalpy were evaluated from the van't Hoff plot presented in Figure 5 and are listed in Table 5.

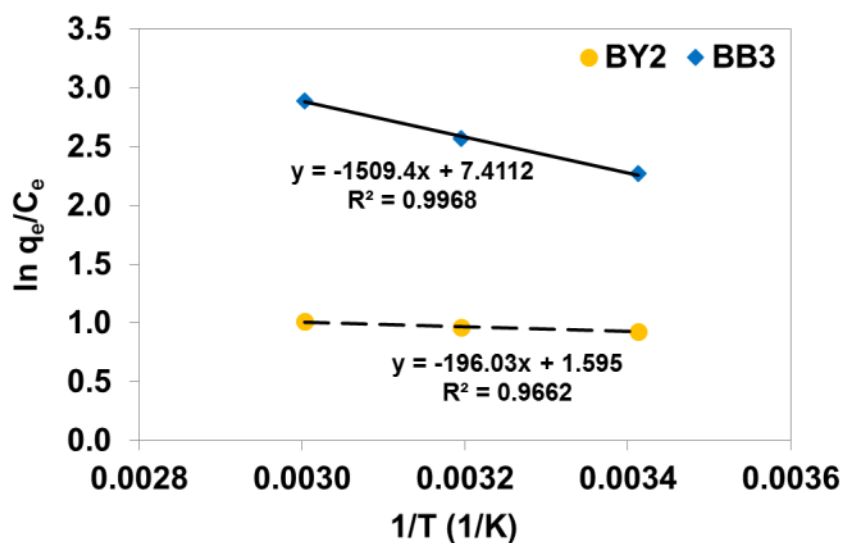


**Figure 5.** The van't Hoff plot for calculation of enthalpy and entropy in BB3-C/SiO<sub>2</sub> and BY2-C/SiO<sub>2</sub> systems.

The negative values of  $\Delta G^\circ$  at 20, 40 and 60 °C show that the sorption process of basic dyes on C/SiO<sub>2</sub> was spontaneous. It was reported previously by Muhammad et al. The authors of [17] studied BY2 removal by PANI/Fe<sub>3</sub>O<sub>4</sub> composite that the  $\Delta G^\circ$  values in the range of  $-20$  to  $0$  kJ/mol show physisorption. The  $\Delta G^\circ$  values were ranged from  $-27.1$  to  $-22.4$  kJ/mol for BB3-C/SiO<sub>2</sub> systems and from  $-21.9$  to  $-19.2$  kJ/mol for BY2 adsorption on C/SiO<sub>2</sub>, which suggest spontaneous and physical adsorption. The positive values of  $\Delta H^\circ$  confirmed endothermic nature of the process. The values of  $\Delta H^\circ$  below 84 kJ/mol also indicates physical nature of interactions between adsorbates and adsorbent [17]. The adsorption enthalpy change for BB3 is larger than that of BY2. It means that the interactions between BB3 and C/SiO<sub>2</sub> surface is stronger and leads to an enhanced adsorption. Moreover, the positive  $\Delta S^\circ$  values 61.6 kJ/mol and 13.3 kJ/mol for

BB3 and BY2, respectively) implied irregular increase in randomness at C/SiO<sub>2</sub>—basic dyes interface during adsorption.

**Table 5.** Thermodynamic parameters of BB3 and BY2 adsorption on C/SiO<sub>2</sub> composite.

T (°C)	K <sub>c</sub> (L/g)	ΔH <sup>o</sup> (kJ/mol)	ΔS <sup>o</sup> (kJ/mol)	ΔG <sup>o</sup> (kJ/mol)
<b>BB3</b>				
20	9.7	12.6	61.6	−22.4
40	13.0			−24.7
60	17.9			−27.1
<b>BY2</b>				
20	2.6	1.6	13.3	−19.2
40	2.5			−20.4
60	2.7			−21.9

### 3.3. Phase Contact Time and Surfactant Impact on Basic Dye Adsorption

The uptake of BB3 and BY2 from aqueous solutions of the initial concentration of dye 100 mg/L as a function of contact time is shown in Figure 6.

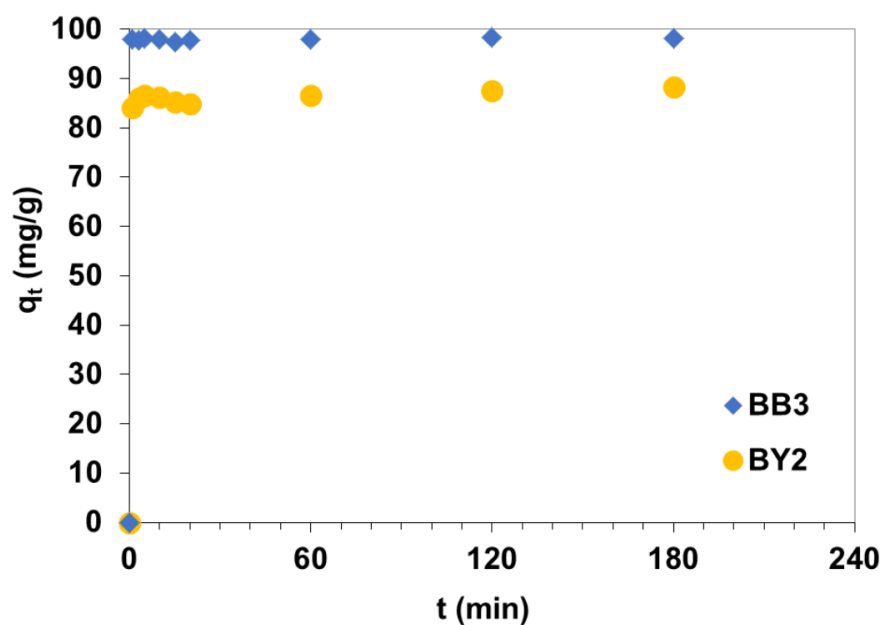


**Figure 6.** Influence of phase contact time on BB3 and BY2 uptake by C/SiO<sub>2</sub> from aqueous solutions of the initial concentration 100 mg/L.

The dye removal rate was very rapid initially and then equilibrium was reached and no significant increase in the rate of removal was observed. During 5 min of phase contact time more than 98% of BB3 ( $q_t = 98.1$  mg/g) and 86% ( $q_t = 86.59$  mg/g) of BY2 was uptaken by C/SiO<sub>2</sub>. The amounts of BB3 and BY2 adsorbed at equilibrium were found to be 98.5 mg/g for BB3 and 88.3 mg/g for BY2. The time necessary to reach the saturation was 60 min for the systems under discussion. The equilibrium time of 50 mg/L BB3 adsorption was reached within 50 to 60 min for Fe<sub>3</sub>O<sub>4</sub>, PANI, and PANI/Fe<sub>3</sub>O<sub>4</sub> composite [17]. The amount of BB3 retained by the sulfuric acid activated montmorillonite mineral increased reached the maximum value (85–99 mg/g for different initial pH values) after approximately 60 min. Goscianska et al. The author of [31] reported that the time necessary to reach dynamic equilibrium during 75 mg/L BY2 adsorption onto the mesoporous carbons of regular structure subjected to oxidation by ammonium persulfate at 30, 60 or 100 °C was 100 min.

In the textile industry, surfactants are used as antistatic, untangling and softening agents in different processes of textile manufacturing such as scouring, dyeing and finishing. In the aforementioned textile treatment processes, the surfactant does not bind permanently to the fiber. They enter the wastewaters in the quantities in which they were introduced into the dyeing bath. They are present in wastewater together with dyes and affect the efficiency of their removal, often being a threat to aquatic ecosystems themselves. It was stated that all anionic surfactants are classified harmful for  $LC_{50}$  between 10–100 mg/L while non-ionic surfactants are toxic for  $LC_{50}$  between 1.0 and 10 mg/L [42–44]. Therefore, the important aspect of the paper was to investigate the dyes removal by the composite from the solutions containing 0.25 g/L of surfactants. Figure 7 compare 100 mg/L BB3 or BY2 uptake by C/SiO<sub>2</sub> in the presence of anionic (SDS), cationic (CTAB) and non-ionic (TX100) surfactants.

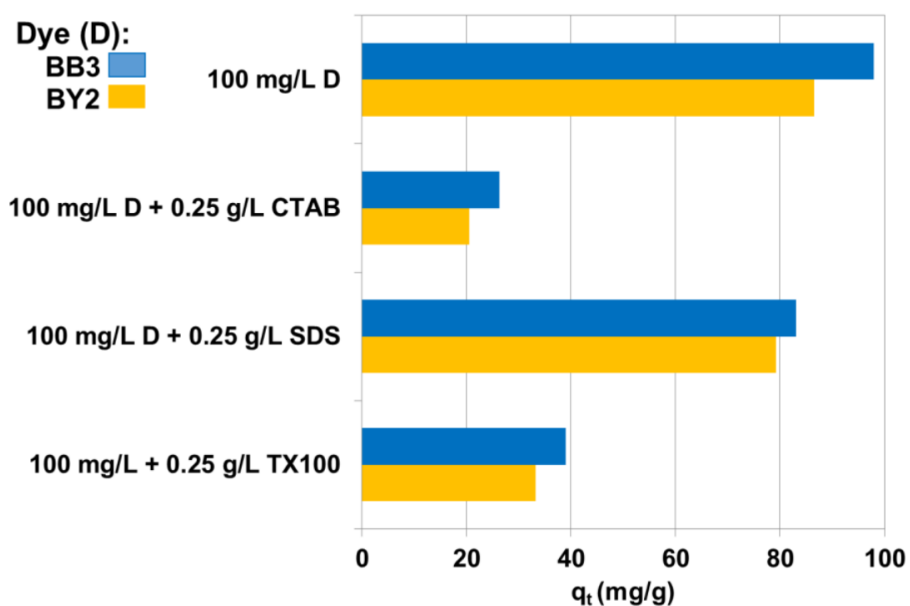


**Figure 7.** Impact of anionic (SDS), cationic (CTAB) and non-ionic (TX100) surfactants on dyes uptake by C/SiO<sub>2</sub>.

There were observed decrease in BB3 and BY2 adsorption in presence of the surfactants. The most noticeable change was observed in the system containing CTAB. The drop of  $q_t$  values in this case can be explained by competitive sorption of cationic surfactant in comparison with cationic dyes. Anionic molecules of SDS interact with cationic dyes. Therefore, the concentration of free dye cations in solution decreases and BB3 and BY2 adsorption decreases. However, this does not preclude the adsorption of dyes-SDS complexes on C/SiO<sub>2</sub> which can be found by electrokinetic studies.

### 3.4. Electrokinetic Results

The solid surface charge density changes as a function of the solution pH in the systems without and with examined dyes and those containing additionally surfactants with different ionic character were presented in Figure 8.

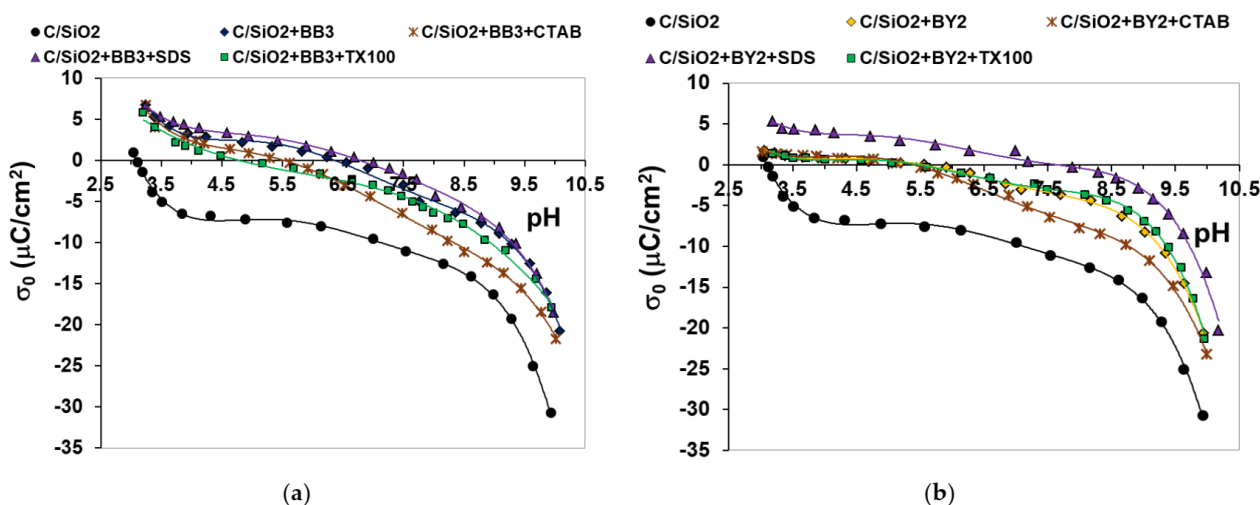


**Figure 8.** (a) Dependencies of the C/SiO<sub>2</sub> surface charge density vs. solution pH in the systems containing BB3 dye and surfactants with different ionic character; (b) Dependencies of the C/SiO<sub>2</sub> surface charge density vs. solution pH in the systems containing BY2 dye and surfactants with different ionic character.

As can be seen in Figure 8, the point of zero charge (pzc) of the examined C/SiO<sub>2</sub> composite without adsorbates is at pH about 3.1. Thus, practically, in the whole examined pH range (above pH 3.1), the solid surface is negatively charged. The adsorption of both dyes causes increase in the solid surface charge density and shift of pzc position towards the higher pH values (i.e., 6.5 for BB3 and 5.5 for BY2). The literature reports confirm that adsorption of small cations causes decrease in  $\sigma_0$  values, because the additional number of negatively charged surface groups are formed [45,46]. However, in the case of relatively big dye molecules, the positive charges in their structure are mostly located in the by-surface layer of the solution in the adsorption layer. This leads to the  $\sigma_0$  increase and such effect is more pronounced for BB3 molecules possessing higher molecular weight. Additionally, besides the electrostatic attraction between negatively charged composite surface and cationic dyes molecules, the hydrogen bonds can be formed between hydroxyl groups of the solid ( $-\text{OH}$ ,  $-\text{OH}_2^+$  and  $-\text{O}^-$ ) and nitrogen atoms in dye molecules [47,48]. The latter phenomenon leads to the exposure of the positive charges of the adsorbed dye molecules towards the bulk phase of the solution, which results in the observed increase in the surface charge density.

In the mixed systems of adsorbates (dye + surfactant), the noticeable changes in the course of  $\sigma_0$  dependencies occur. In the presence of anionic SDS, the further increase in the solid surface charge density (in comparison to the systems containing only dye) takes place (especially in the case of BY2 containing suspensions). In such a case the dye-SDS complexes are formed and they can be adsorbed on the solid surface. The negatively charged heads of anionic surfactant interact with positive charges of dye molecules, and thus such complexes undergo binding with the solid active sites mainly through hydrogen bonds (using for this purpose nitrogen atoms of dye molecules). In such a case the carbon tails of SDS surfactant are oriented towards the solution and the second adsorption layer of anionic surfactant can be formed with anionic heads directed into the solution.

The presence of cationic CTAB and nonionic Triton X-100 decreases significantly the dye adsorbed amounts. Such behavior confirm the competitive adsorption of these surfactants and dye molecules. The addition of nonionic surfactant has minimal effect on the  $\sigma_0$  values in the dye presence, whereas the addition of cationic surfactant resulted in noticeable decrease in the  $\sigma_0$  values in the pH range above pzc (i.e., 6.5 for BB3 and 5.5 for BY2). This proves the effective adsorption of CTAB molecules in the mixed surface layer, which leads to the formation of additional number of negatively charged surface groups [49]. There is the possibility of dye-Triton X-100 complexes formation through hydrophilic-hydrophobic

interactions [50]; nevertheless, they remain mainly in the solution, and adsorption of a small number of them practically does not change the solid surface charge.

The presence of adsorption layers of single and mixed adsorbates on the carbon-silica composite surface influences also the electrokinetic potential. The zeta potential changes as a function of the solution pH in the systems without and with examined dyes, and those containing additionally surfactants with different ionic character were presented in Figure 9. The isoelectric point (iep) for the C/SiO<sub>2</sub> without additives occurs at pH about 3.3, which is in good agreement with the pzc value. The presence of both dyes (the small shift of iep to value of about 4.5 is observed) and dye+Triton X-100 mixed adsorbates changes inconsiderably the zeta potential of the solid particles. The changes in the zeta potential in the examined systems are the resultant of three phenomena accompanying the adsorption process: ionic character of adsorbate, shift of slipping plane from the solid surface and replacement of supporting electrolyte ions from the surface towards the diffuse part of electrical double layer [51].

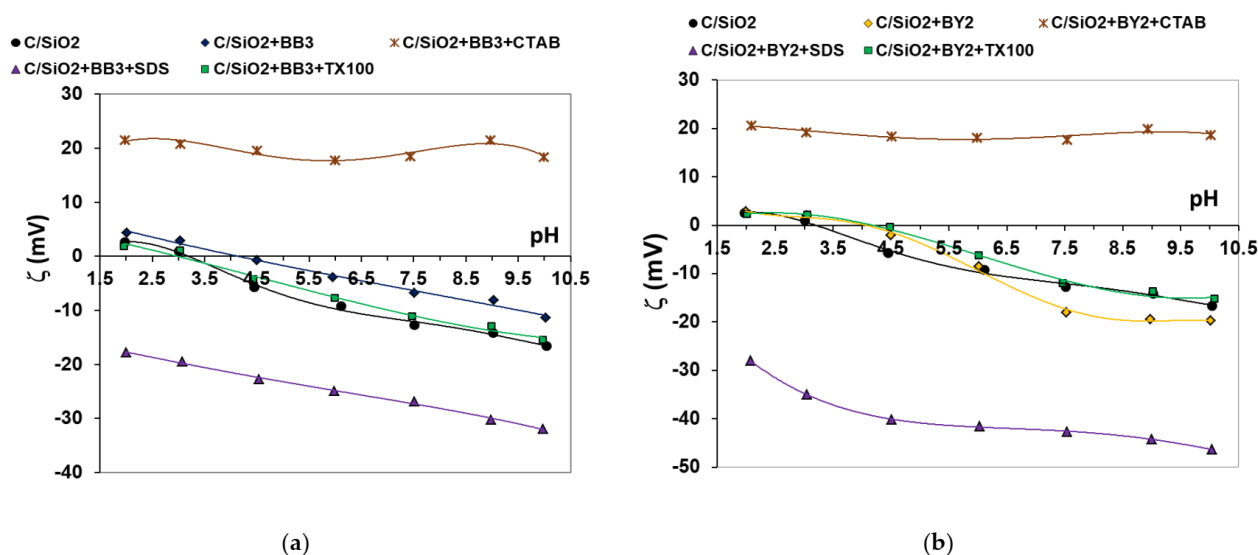


**Figure 9.** (a) Dependencies of the C/SiO<sub>2</sub> zeta potential vs. solution pH in the systems containing BB3 dye and surfactants with different ionic character; (b) Dependencies of the C/SiO<sub>2</sub> zeta potential vs. solution pH in the systems containing BY2 dye and surfactants with different ionic character.

In the case of anionic surfactant presence in the dye adsorption layer, the considerable shift of the slipping plane due to the dye-SDS complexes binding and formation of a second layer of surfactant molecules with anionic heads located in the slipping plane area are the more probable mechanisms of considerable reduction of zeta potential. On the other hand, the pronounced increase in electrokinetic potential in the mixed dye + CTAB adsorbates presence results from preferential adsorption of smaller cationic surfactant molecules (through the positive heads) and creation of CTAB adsorption multilayers with positive charges located in the slipping plane area [52].

#### 4. Conclusions

The carbon-silica composite was applied for the removal of hazardous basic dyes such as C.I. Basic Blue 3 and C.I. Basic Yellow 2 from aqueous solutions. The batch equilibrium studies revealed high adsorption capacity of C/SiO<sub>2</sub> towards dyes at the level of 924.6–1295.9 mg/g for BB3 and 716.3–733.2 mg/g for BY2 depending on temperature. There was observed increase in the adsorption capacity with increasing temperature in the BB3-C/SiO<sub>2</sub> system. The Freundlich isotherm model describes equilibrium data better than Langmuir or Temkin ones. The physical nature of adsorption process was confirmed by the negative values of free energy and positive values of enthalpy. Additives such as anionic, cationic and non-ionic surfactants in the amount of 0.25 g/L reduced basic dyes

adsorption on the composite surface. The adsorption of both dyes causes considerable increase in the solid surface charge density and noticeable increase in the zeta potential of C/SiO<sub>2</sub> particles. The changes in electrokinetic parameters in mixed dye + surfactant systems of adsorbates proved the physical nature of their adsorption on the composite surface, mainly through hydrogen bonds. The specific structure of adsorption layers results on slipping plane shift and changes in ionic composition of surface and diffuse parts of electrical double layer formed at the solid/liquid interface.

Considering the above, the C/SiO<sub>2</sub> composite can be considered as an effective adsorbent of impurities, including basic dyes from textile effluents or dyeing baths containing surfactants.

**Author Contributions:** Conceptualization, M.W. (Małgorzata Wiśniewska), M.W. (Monika Wawrzkiwicz), V.B.; methodology, M.W. (Małgorzata Wiśniewska), M.W. (Monika Wawrzkiwicz), A.N.-W., V.B.; software, M.W. (Małgorzata Wiśniewska), M.W. (Monika Wawrzkiwicz); validation, M.W. (Małgorzata Wiśniewska), M.W. (Monika Wawrzkiwicz) and A.N.-W.; formal analysis, M.O., M.M.; investigation, M.O., M.M.; resources, M.W. (Małgorzata Wiśniewska) and A.N.-W.; data curation, M.O., M.M.; writing—original draft preparation, M.W. (Małgorzata Wiśniewska), M.W. (Monika Wawrzkiwicz); writing—review and editing, M.W. (Małgorzata Wiśniewska), M.W. (Monika Wawrzkiwicz), A.N.-W.; visualization, M.W. (Małgorzata Wiśniewska), M.W. (Monika Wawrzkiwicz); supervision, M.W. (Małgorzata Wiśniewska), M.W. (Monika Wawrzkiwicz); All authors have read and agreed to the published version of the manuscript.

**Funding:** This research received no external funding.

**Institutional Review Board Statement:** Not applicable.

**Informed Consent Statement:** Not applicable.

**Data Availability Statement:** The data presented in this study are available in this article.

**Conflicts of Interest:** The authors declare no conflict of interest.

## References

1. Upadhyay, K.K.; Pandey, A.C.; Manzoor, J. Impact of Dyes on the Chemistry of Water and its Implications: A Review. *Bio Bull.* **2017**, *3*, 1–7.
2. Berradi, M.; Hsissou, R.; Khudhair, M.; Assouag, M.; Cherkaoui, O.; El Bachiri, E.; El Harfi, A. Textile finishing dyes and their impact on aquatic environs. *Helyion* **2019**, *5*, e02711. [[CrossRef](#)]
3. Hynes, N.R.J.; Kumar, J.S.; Kamyab, H.; Sujana, J.A.J.; Al-Khashman, O.A.; Kuslu, Y.; Ene, A.; Kumar, B.S. Modern enabling techniques and adsorbents based dye removal with sustainability concerns in textile industrial sector—A comprehensive review. *J. Clean. Prod.* **2020**, *272*, 122636. [[CrossRef](#)]
4. Tofighy, M.A.; Mohammadi, T. Adsorption of divalent heavy metal ions from water using carbon nanotube sheets. *J. Hazard. Mater.* **2011**, *185*, 140–147. [[CrossRef](#)] [[PubMed](#)]
5. Thamer, B.M.; Aldalbahi, A.; Moydeen, M.; Al-Enizi, A.M.; El-Hamshary, H.; Singh, M.; Bansal, V.; El-Newehy, M.H. Alkali-activated electrospun carbon nanofibers as an efficient bifunctional adsorbent for cationic and anionic dyes. *Colloids Surf. A* **2019**, *582*, 123835. [[CrossRef](#)]
6. Zhang, Y.; Ou, H.; Liu, H.; Ke, Y.; Zhang, W.; Liao, G.; Wang, D. Polyimide-based carbon nanofibers: A versatile adsorbent for highly efficient removals of chlorophenols, dyes and antibiotics. *Colloids Surf. A* **2018**, *537*, 92–101. [[CrossRef](#)]
7. Konicki, W.; Aleksandrak, M.; Moszyński, D.; Mijowska, E. Adsorption of anionic azo-dyes from aqueous solutions onto graphene oxide: Equilibrium, kinetic and thermodynamic studies. *J. Colloid Interface Sci.* **2017**, *496*, 188–200. [[CrossRef](#)]
8. Boruah, P.K.; Sharma, B.; Hussain, N.; Das, M.R. Magnetically recoverable Fe<sub>3</sub>O<sub>4</sub>/graphene nanocomposite towards efficient removal of triazine pesticides from aqueous solution: Investigation of the adsorption phenomenon and specific ion effect. *Chemosphere* **2017**, *168*, 1058–1067. [[CrossRef](#)]
9. Yu, F.; Ma, J.; Bi, D. Enhanced adsorptive removal of selected pharmaceutical antibiotics from aqueous solution by activated graphene. *Environ. Sci. Pollut. Res.* **2015**, *22*, 4715–4724. [[CrossRef](#)]
10. Wiśniewska, M.; Nowicki, P. Peat-based activated carbons as adsorbents for simultaneous separation of organic molecules from mixed solution of poly(acrylic acid) polymer and sodium dodecyl sulfate surfactant. *Colloids Surf. A* **2020**, *585*, 124179. [[CrossRef](#)]
11. Szewczuk-Karpisz, K.; Wiśniewska, M.; Nowicki, P.; Oleszczuk, P. Influence of protein internal stability on its removal mechanism from aqueous solutions using eco-friendly horsetail herb-based engineered biochar. *Chem. Eng. J.* **2020**, *388*, 124156. [[CrossRef](#)]
12. Yang, X.; Wan, Y.; Zheng, Y.; He, F.; Yu, Z.; Huang, J.; Gao, B. Surface functional groups of carbon-based adsorbents and their roles in the removal of heavy metals from aqueous solutions: A critical review. *Chem. Eng. J.* **2019**, *366*, 608–621. [[CrossRef](#)]

13. Szewczuk-Karpisz, K.; Wiśniewska, M.; Medykowska, M.; Galaburda, M.V.; Bogatyrov, V.M.; Oranska, O.I.; Błachnio, M.; Oleszczuk, P. Simultaneous adsorption of Cu(II) ions and poly(acrylic acid) on the hybrid carbon-mineral nanocomposites with metallic elements. *J. Hazard. Mater.* **2021**, *412*, 125138. [[CrossRef](#)]
14. Szewczuk-Karpisz, K.; Wiśniewska, M.; Medykowska, M.; Bogatyrov, V.; Sokołowska, Z. Adsorption layer structure on the surface of carbon-silica composite in the presence of proteins of different internal stability and Cu(II) ions—The effect on solid aggregation. *J. Mol. Liq.* **2020**, *309*, 113072. [[CrossRef](#)]
15. Szewczuk-Karpisz, K.; Bogatyrov, V.M.; Galaburda, M.; Sokołowska, Z. Study on Adsorption and Aggregation in the Mixed System of Polyacrylamide, Cu(II) Ions and Innovative Carbon–Silica Composite. *Polymers* **2020**, *12*, 961. [[CrossRef](#)]
16. Lellis, B.; Fávoro-Polonio, C.Z.; Pamphile, J.A.; Polonio, J.C. Effects of textile dyes on health and the environment and bioremediation potential of living organisms. *Biotechnol. Res. Innov.* **2019**, *3*, 275. [[CrossRef](#)]
17. Muhammad, A.; Shah, A.H.A.; Bilal, S.; Rahman, G. Basic blue dye adsorption from water using polyaniline/magnetite (Fe<sub>3</sub>O<sub>4</sub>) composites: Kinetic and thermodynamic aspects. *Materials* **2019**, *12*, 1764. [[CrossRef](#)]
18. Foo, K.Y.; Hameed, B.H. Insights into the modeling of adsorption isotherm systems. *Chem. Eng. J.* **2010**, *156*, 2–10. [[CrossRef](#)]
19. Marković, D.D.; Lekić, B.M.; Rajaković-Ognjanović, V.N.; Onjia, A.E.; Rajaković, L.V. A new approach in regression analysis for modeling adsorption isotherms. *Sci. World J.* **2014**, *2014*, 930879. [[CrossRef](#)]
20. Sivarajasekar, N.; Baskar, R. Adsorption of Basic Magenta II onto H<sub>2</sub>SO<sub>4</sub> activated immature *Gossypium hirsutum* seeds: Kinetics, isotherms, mass transfer, thermodynamics and process design. *Arab. J. Chem.* **2019**, 1322–1337. [[CrossRef](#)]
21. Liu, Y. Is the free energy change of adsorption correctly calculated? *J. Chem. Eng. Data* **2009**, *54*, 1981–1982. [[CrossRef](#)]
22. Janusz, W. Electrical double layer at metal oxide-electrolyte interface. In *Interfacial Forces and Fields Theory and Applications*; Dekker, M., Ed.; CRC Pres: New York, NY, USA, 1999.
23. Oshima, H. A simple expansion for Henry's function for the retardation effect in electrophoresis of spherical colloidal particles. *J. Colloid Interface Sci.* **1994**, *168*, 269–271. [[CrossRef](#)]
24. Siew-Teng, O.; Suat-Yen, T.; Eng-Cheong, K.; Siew-Ling, L.; Sie-Tiong, H. Equilibrium studies for Basic blue 3 adsorption onto durian peel (*Durio zibethinus* Murray). *Desal. Water Treat.* **2012**, *45*, 161. [[CrossRef](#)]
25. Crini, G.; Gimbert, F.; Robert, C.; Martel, B.; Adam, O.; Morin-Crini, N.; Badot, P.-M. The removal of Basic Blue 3 from aqueous solutions by chitosan-based adsorbent: Batch studies. *J. Hazard. Mater.* **2008**, *153*, 96. [[CrossRef](#)]
26. Taşar, Ş.; Kaya, F.; Özer, A. Adsorption of C.I. Basic Blue 3 dye molecules from aqueous media by sulfuric acid-activated montmorillonite mineral. *J. Turk. Chem. Soc. B* **2017**, *1*, 1.
27. Öztürk, A.; Malkoc, E. Adsorptive potential of cationic Basic Yellow 2 (BY2) dye onto natural untreated clay (NUC) from aqueous phase: Mass transfer analysis, kinetic and equilibrium profile. *Appl. Surf. Sci.* **2014**, *299*, 105. [[CrossRef](#)]
28. Öztürk, A.; Malkoc, E. Cationic Basic Yellow 2 (BY2) adsorption onto manure ash: Surface properties and adsorption mechanism. *Desal. Water Treat.* **2014**, *54*, 209. [[CrossRef](#)]
29. Aber, S.; Eshfahlan, F.H. Removal of C.I. Basic Yellow 2 from aqueous solution by adsorption onto granular activated carbon using an on-line spectrophotometric analysis system: Kinetic and equilibrium study. *Glob. NEST J.* **2011**, *13*, 246.
30. Mall, I.D.; Srivastava, V.C.; Agarwal, N.K. Adsorptive removal of Auramine-O: Kinetic and equilibrium study. *J. Hazard. Mater.* **2007**, *143*, 386. [[CrossRef](#)]
31. Goscińska, J.; Marciniak, M.; Pietrzak, R. The effect of surface modification of mesoporous carbons on Auramine-O dye removal from water. *Adsorption* **2015**, *22*, 531. [[CrossRef](#)]
32. Nwafor, N.P.; Moutloali, R.M.; Sikhwivhilu, K.; Filoni, O.B.; Adams, L.A. Antifouling polyethersulfone-petrol soot nanoparticles composite ultrafiltration membrane for dye removal in wastewater. *Membranes* **2021**, *11*, 361. [[CrossRef](#)]
33. Ahmed, I.A.; Ragab, A.H.; Habila, M.A.; Alomar, T.S.; Aljuhani, E.H. Equilibrium and kinetic study of anionic and cationic pollutants remediation by limestone—Chitosan—alginate nanocomposite from aqueous solution. *Molecules* **2021**, *26*, 2586. [[CrossRef](#)]
34. Spoială, A.; Ilie, C.-I.; Ficai, D.; Ficai, A.; Andronescu, E. Chitosan-based nanocomposite polymeric membranes for water purification—a review. *Materials* **2021**, *14*, 2091. [[CrossRef](#)]
35. Kadhim, R.J.; Al-Ani, F.H.; Al-shaeli, M.; Alsahy, Q.F.; Figoli, A. Removal of dyes using graphene oxide (GO) mixed matrix membranes. *Membranes* **2020**, *10*, 366. [[CrossRef](#)]
36. Marotta, A.; Luzzi, E.; Salzano de Luna, M.; Aprea, P.; Ambrogi, V.; Filippone, G. Chitosan/zeolite composite aerogels for a fast and effective removal of both anionic and cationic dyes from water. *Polymers* **2021**, *13*, 1691. [[CrossRef](#)]
37. Kashefi Alasl, M.; Khosravi, M.; Marandi, R.; Seyedi, K.; Khataei, A.R. Investigation of Basic Yellow 2 removal from contaminated water by electrocoagulation method in the batch reactor. *J. Environ. Sci. Technol.* **2005**, *26*, 78–97.
38. Hmani, E.; Samet, Y.; Abdelhédi, R. Electrochemical degradation of auramine-O dye at boron-doped diamond and lead dioxide electrodes. *Diam. Relat. Mater.* **2012**, *30*, 1–8. [[CrossRef](#)]
39. Montazerzohori, M.; Nasr-Esfahani, M.; Moradi-Shammi, Z.; Malekhoseini, A. Photocatalytic decolorization of auramine and its kinetics study in the presence of two different sizes titanium dioxide nanoparticles at various buffer and non-buffer media. *J. Industr. Eng. Chem.* **2015**, *21*, 1044–1050. [[CrossRef](#)]
40. Özcan, A.; Şahin, Y.; Koparal, S.; Oturan, M.A. Electro-Fenton removal of the cationic dye Basic Blue 3 by using carbon felt cathode. *Environ. Eng. Manag. J.* **2009**, *19*, 267–275.



41. Khataee, A.; Taseidifar, M.; Sheydaei, M.; Khorram, S.; Woo Joo, S. Sonocatalytic degradation of Basic Blue 3 using plasma-treated magnetite nanostructures. *Curr. Nanosci.* **2015**, *12*, 125–134. [[CrossRef](#)]
42. Dhaif-Allah, M.A.H.; Taqui, S.N.; Syed, U.T.; Syed, A.A. Kinetic and isotherm modeling for acid blue 113 dye adsorption onto low-cost nutraceutical industrial fenugreek seed spent. *App. Water Sci.* **2020**, *10*, 58. [[CrossRef](#)]
43. El-Azazy, M.; El-Shafie, A.S.; Ashraf, A.; Issa, A.A. Eco-structured biosorptive removal of Basic Fuchsin using pistachio nutshells: A definitive screening design-based approach. *Appl. Sci.* **2019**, *9*, 4855. [[CrossRef](#)]
44. Jahan, K.; Balzer, S.; Mosto, P. Toxicity of nonionic surfactants. *WIT Trans. Ecol. Environ.* **2008**, *110*, 281. [[CrossRef](#)]
45. Skwarek, E.; Janusz, W. Adsorption of Cd(II) ions at the hydroxyapatite/electrolyte solution interface. *Adsorption* **2016**, *51*, 11–21. [[CrossRef](#)]
46. Skwarek, E.; Janusz, W. Study of sorption processes of strontium on the synthetic hydroxyapatite. *Adsorption* **2016**, *22*, 697–706.
47. Kasprzyk-Hordern, B. Chemistry of alumina, reactions in aqueous solution and its application in water treatment. *Adv. Colloid Interf. Sci.* **2004**, *110*, 19–48. [[CrossRef](#)]
48. Wiśniewska, M.; Chibowski, S.; Urban, T.; Sternik, D. Investigation of the alumina properties with adsorbed polyvinyl alcohol. *J. Therm. Anal. Calorim.* **2011**, *103*, 329–337. [[CrossRef](#)]
49. Wawrzekiewicz, M.; Wiśniewska, M.; Gun'ko, V.M.; Zarko, V.I. Adsorptive removal of acid, reactive and direct dyes from aqueous solutions and wastewater using mixed silica-alumina oxide. *Powder Tech.* **2015**, *278*, 306–315. [[CrossRef](#)]
50. Wiśniewska, M.; Nowicki, P.; Urban, T. Influence of surfactants with different ionic character on the structure of poly(acrylic acid) adsorption layer on the activated biocarbons surface—Electrokinetic and stability studies. *J. Mol. Liq.* **2021**, *332*, 115872. [[CrossRef](#)]
51. M'Pandou, A.; Siffert, B. Polyethylene glycol adsorption at the TiO<sub>2</sub>-H<sub>2</sub>O interface: Distortion of ionic structure and shear plane position. *Colloids Surf. A* **1987**, *4*, 159–172. [[CrossRef](#)]
52. Hunter, R.J. *Zeta Potential in Colloid Science*; Academic Press: New York, NY, USA, 1981.